Superexchange in manganese formate dihydrate, studied by polarized-neutron diffraction

1993 J. Phys.: Condens. Matter 5 6447

(http://iopscience.iop.org/0953-8984/5/35/010)

J. Phys.: Condens. Matter 5 (1993) 6447–6460. Printed in the UK

Superexchange in manganese formate dihydrate, studied by polarized-neutron diffraction

P Radhakrishna†‡, B Gillon† and G Chevrier†§

† Laboratoire Léon Brillouin (CEA–CNRS), Centre d'Etudes Nucléaires Saclay, 91191 Gif-sur-Yvette, France

‡ Jawaharlal Nehru Centre for Advanced Scientific Research, I I Sc Campus, Bangalore 560012, India

Received 23 November 1992, in final form 22 April 1993

Abstract. The crystalline structure of manganese formate dihydrate $Mn(HCOO)_2 \cdot 2H_2O$ may be described by stacking along the a axis two parallel layers of non-equivalent manganese Mn^{2+} ions, consisting of antiferromagnetically coupled A ions and weakly interacting B ions. The A layers are characterized by formate bridges relating each A ion to the four neighbouring ions, while the B ions are isolated from each other. On the other hand, the A layers are related to the B layers by formate bridges. The induced magnetization density has been determined by polarized-neutron diffraction, slightly above (and below) the antiferromagnetic (AF) ordering temperature $T_N = 3.7$ K. A field of 0.8 T was applied to the single crystal along b. In our experimental conditions, below T_N the AF moments of the A ions are canted, with a weak ferromagnetic component along b.

Magnetic moments are observed on the carbon and oxygen atoms of the A–A and A–B formate bridges, demonstrating the role of the formate group in the indirect exchange magnetic interaction between A ions. At 5.5 K, alternate positive and negative signs are found on the O–C–O pathway between two A ions and between the A and B ions: O(1)(0.022(6)μ_B)–C(1)(−0.017(7)μ_B)–O(2)(0.015(6)μ_B) and O(3)(0.024(7)μ_B)–C(2)(−0.011(9)μ_B)–O(4)(0.013(7)μ_B). The induced moments on A and B are equal to 0.38(2)μ_B and 1.73(2)μ_B, respectively.

At 2.5 K, the measurements have been confined to the reflections with $k + l$ even, which do not contain any contribution from the AF components. The magnetization density observed around the A ions is then the sum of the spontaneous weak ferromagnetic component (0.09μ_B) and of the component induced by the field (0.19μ_B). The spin distribution on the bridges is perturbed in the magnetically ordered phase; in particular, the alternation of signs is no longer observed.

1. Introduction

Manganese formate dihydrate has a monoclinic crystal structure with two manganese ions in non-equivalent crystalline sites, which show totally different magnetic behaviours. The A ions in site (0, 0, 0) are related by formate bridges and form layers piled up along the a axis [1]. These layers are separated from each other by parallel layers of manganese ions in site B (0.5, 0.5, 0) as illustrated in figure 1. The B ions are isolated from each other, but each B ion is related to an A ion through a formate bridge.

A three-dimensional antiferromagnetic (AF) ordering of the A moments takes place at $T_N = 3.7$ K, as shown by magnetic susceptibility measurements and magnetic resonance studies [2–5] and confirmed by neutron powder diffraction [6]. Two-dimensional AF

§ Author to whom correspondence should be addressed.

0953-8984/93/356447+14$07.50

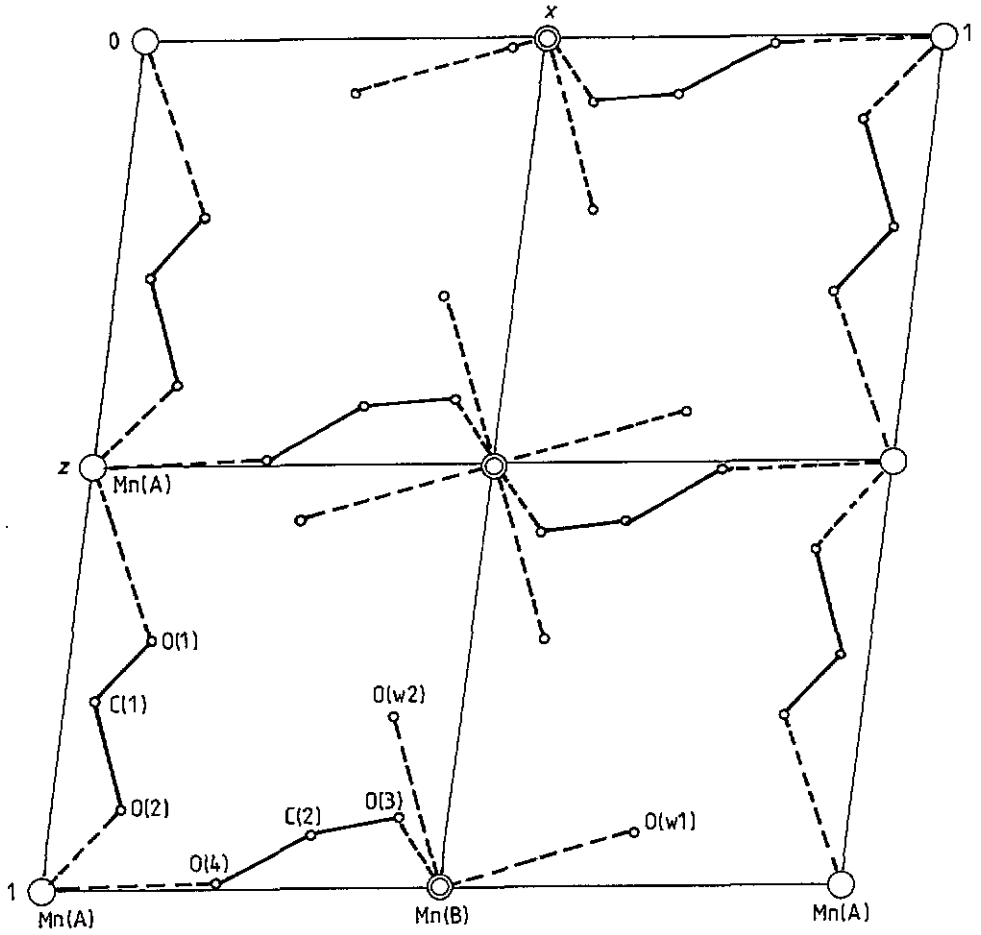

Figure 1. Projection of the crystallographic structure of $Mn(HCOO)_2 \cdot 2H_2O$ along the c direction.

correlations between the A ions have been observed by neutron scattering in the range $3.7\ K < T < 7.8\ K$ [7].

The susceptibility curve measured on a single crystal shows, below the peak at $T_N = 3.7$ K, a second sharp peak at $T_0 = 1.7$ K [3,8]. The existence of a weak ferromagnetic component in the AF state has been shown by torque measurement; the transition at 1.7 K corresponds to a reorientation of this component from the c to the b direction, with an increase in magnitude from $0.017\mu_B$ to $0.095\mu_B$ per Mn ion at low temperatures [9]. The magnetic structures in zero field above (type I) and below 1.7 K (type II) are illustrated in figure 2. A transition from the type I to the type II structure may be induced in the temperature range $1.7\ K < T < 3.7$ K by applying an external magnetic field along the crystallographic b direction; at 2.5 K, a field of 0.4 T induces spin flop [10].

Below 1.7 K, the behaviour of the susceptibility suggests that half the ions are still paramagnetic [11]. The specific heat measurement confirms this conclusion [12]. The B ions remain paramagnetic down to a very low temperature, AF ordering occurring at 0.6 K [11, 13]. Recent proton NMR measurements have permitted the susceptibilities of the two subsystems to be observed separately [14].

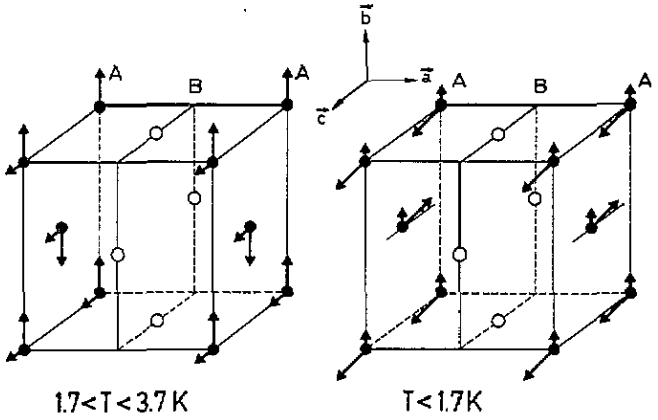

Figure 2. Magnetic structure of manganese formate dihydrate in zero field: for type I at 3.7 K > T > 1.7 K; for type II at T < 1.7 K.

The coupling between A ions can be explained by superexchange via the formate bridges which bind each A to four other A ions in the layers and two A ions of the next A layers via the A–B formate bridges [2]. This implies the existence of a moment on the formate group due to its interaction with the Mn^{2+} ion:

$$\begin{array}{l} \quad\ \ \mathrm{H} \\ \quad\ \ | \\ \mathrm{O}=\mathrm{C}-\mathrm{O}^{-}. \end{array}$$

Polarized-neutron diffraction has been shown to be a very powerful technique for the study of the delocalization effect from metal to organic ligands [15] as well as weak ferromagnetism [16]. We report the determination of the magnetization density in $Mn(HCOO)_2 \cdot 2H_2O$ and discuss the role of the formate bridge in the mechanism of indirect magnetic interaction between the manganese ions.

2. Experimental details

2.1. Experimental method

The sensitivity of polarized-neutron diffraction allows one to determine very weak magnetic structure factors, from which the magnetization density in the crystallographic cell can be deduced. This magnetization density is induced in the sample by applying a vertical magnetic field in order to align the magnetic moments of the unpaired electrons.

In the paramagnetic state, the total moment which is induced in the sample, of magnetic susceptibility χ, along the field direction of magnitude H, is equal to

$$M = \chi H.$$

In the AF state, in the case of weak ferromagnetism, the induced total moment is given by

$$M = M_{\text{spontaneous}} + \chi_{\perp} H$$

where $\chi_{\perp}$ is the magnetic susceptibility and H the applied magnetic field.

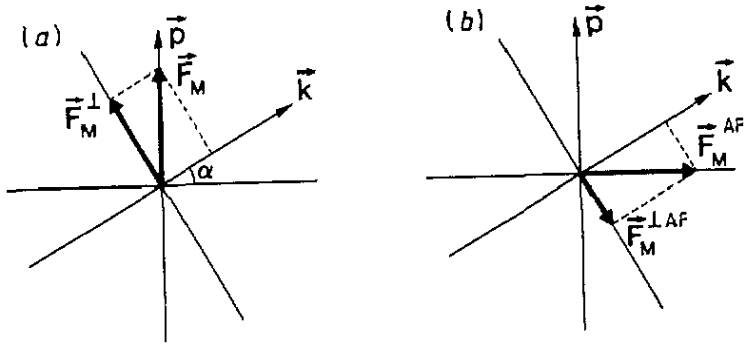

Figure 3. Relative geometry of the polarization and magnetic structure factors: (*a*) induced component along the vertical field; (*b*) AF component perpendicular to the field.

The magnetic structure factors are the Fourier components of the magnetization density $\rho(\boldsymbol{r})$, which is the sum of the contributions due to the spin and the orbital moments of the magnetic electrons. In the case of the S-state ion Mn^{2+} ($S = \frac{5}{2}$), the orbital moment is quenched, and the magnetization density is due to spin only. The magnetic structure factor of a Bragg reflection with scattering vector $\boldsymbol{K}$ can be written as a discrete sum over the atoms in the cell, assuming that the electronic unpaired spins are localized on the magnetic atoms:

$$\boldsymbol{F}_M(\boldsymbol{K}) = \sum_i s_i m_i f_M^i(\boldsymbol{K}) \exp(-2i\pi \boldsymbol{K} \cdot \boldsymbol{r}_i) \tag{1}$$

where m_i is the magnetic moment on atom i, with direction defined by the unit vector s_i and $f_M^i(\boldsymbol{K})$ is the magnetic form factor relative to atom i.

The magnetic scattering amplitude for a Bragg reflection with scattering vector $\boldsymbol{K}$ is proportional to the component $\boldsymbol{F}_M^{\perp}$ of the magnetic structure factor $\boldsymbol{F}_M$ perpendicular to $\boldsymbol{K}$:

$$\boldsymbol{F}_M^{\perp} = \boldsymbol{K} \times \boldsymbol{F}_M \times \boldsymbol{K}.$$

The polarized-neutron diffraction technique consists in measuring the intensity ratio of I_+ to I_- diffracted at each Bragg peak for incident neutrons polarized in the vertical direction with spin up or down, respectively. This flipping ratio can be written, in the case of a centrosymmetric space group, in terms of the magnetic and nuclear structure factors $\boldsymbol{F}_M^{\perp}$ and F_N:

$$R = I_+/I_- = (F_N^2 + 2F_N\boldsymbol{F}_M^{\perp} \cdot \boldsymbol{p} + F_M^{\perp 2})/(F_N^2 - 2eF_N\boldsymbol{F}_M^{\perp} \cdot \boldsymbol{p} + F_M^{\perp 2}) \tag{2}$$

where $\boldsymbol{p}$ is a vector representing the beam polarization (with magnitude p), and e the flipping efficiency.

In the paramagnetic domain and in the absence of any magnetic anisotropy, the induced magnetic moments are parallel to the external field, which is parallel to the neutron polarization $\boldsymbol{p}$; in this case $\boldsymbol{F}_M$ and $\boldsymbol{p}$ are collinear as shown in figure 3(*a*), and equation (2) becomes

$$R = I_+/I_- = (F_N^2 + 2pq^2F_NF_M + q^2F_M^2)/(F_N^2 - 2epq^2F_NF_M + q^2F_M^2) \tag{3}$$

where $q^2 = \sin^2\alpha$, α being the angle between the direction of the magnetic moment in the sample and the scattering vector.

Equation (3) is usually written as a function of the ratio $\gamma = F_M/F_N$. This leads to a quadratic equation in γ, one solution of which only generally has a physical meaning, and the magnetic structure factor is then given by $F_M = \gamma F_N$.

In the case where an AF component exists at the same time as a nuclear Bragg reflection, which occurs at $T < 3.7$ K for manganese formate dihydrate for certain types of reflection, the general expression has to be considered. In the type II structure shown in figure 2, which takes place for a field $H \| b$ larger than 0.4 T, the AF structure factor F_M^{AF} is perpendicular to the applied field, which means also to the polarization p. In this case the scalar product of p and the component $F_M^{\perp AF}$ perpendicular to the scattering vector is not zero for out-of-plane reflections as illustrated in figure 3(*b*) [17]. For these reflections, a term due to the AF component then has to be taken into account. In the following study, the measurement of such reflections has been excluded in order to avoid the problem of sharing between AF and ferromagnetic or induced contributions.

2.2. *Structure determination at 20 K*

The determination of the magnetic structure factors requires knowledge of the nuclear structure factors under the same experimental conditions. This is why a single-crystal structure determination by neutron diffraction at low temperatures needed to be performed preliminarily to the polarized-neutron study.

Manganese formate dihydrate crystallizes in the monoclinic system $P2_1/c$, with $Z = 4$, $a = 8.86$ Å, $b = 7.29$ Å, $c = 9.6$ Å and $\beta = 97.7°$ at room temperature [1]. The positions of the hydrogen atoms at room temperature have been previously determined by a neutron diffraction study [18]. In order to obtain the precise structure at low temperatures, we have performed a neutron diffraction experiment on a single crystal at 20 K on the four-circle diffractometer 5C2, on the hot source at the Laboratoire Léon Brillouin (LLB), Saclay. The dimensions of the sample were 6 mm × 5 mm × 3 mm.

The experimental data and refinement conditions are reported in table 1. The cell parameters given in table 1 were refined from 19 reflections at 20 K. Equivalent reflections (hkl) and $(h\bar{k}l)$ were collected. The integrated intensities were corrected for the Lorentz factor and for absorption with a linear coefficient $\mu = 1.87$ cm^{-1}. The least-squares refinement program PROMETHEUS [19] has been used to refine the position and thermal parameters. Anisotropic thermal factors have been refined other than for the manganese atoms. The coefficient g has been refined in order to account for extinction effects. Only reflections with $F > 3\sigma$ were used in the refinement. A reliability factor of 0.062 was obtained. The position parameters and equivalent isotropic thermal coefficients are listed in table 2.

Each manganese is surrounded by six oxygen atoms, in a nearly octahedral configuration. The distances between one manganese ion and the neighbouring oxygen atoms vary from 2.144 to 2.219 Å. The A ion is related to six formate bridges with respective Mn–O distances: 2.170(7) Å for Mn–O(1), 2.148(4) Å for Mn–O(2) and 2.190(4) Å for Mn–O(4). The B ion is related to the two formate bridges, with Mn–O(3) equal to 2.219(4) Å, and has four neighbouring water molecules, with distances Mn–O(5) of 2.193(5) Å and Mn–O(6) of 2.144(7) Å.

The length of the C–O bond in the formate bridges is almost constant: 1.249(5) Å for both CO bonds in the A–A bridge and C(2)–O(3) = 1.246(4) Å, C(2)–O(4) = 1.258(4) Å for the A–B bridge.

Table 1. Experimental data and refinement conditions for the structure determination at 20 K.

	Value at low temperature (this work)
a (Å)	8.774(16)
b (Å)	7.171(12)
c (Å)	9.611(32)
β (deg)	98.13(22)
T (K)	20
Wavelength (Å)	0.833
Measured reflections	2571
Independent reflections ($F > 3\sigma$)	1138
Extinction coefficient $g \times 10^4$	0.040
Number of variables	130
Goodness of fit χ^2	2.72
Agreement factor $R_W(F)$	0.062

Table 2. Refined position and thermal parameters at 20 K. The equivalent isotropic thermal factor is defined by $B_{eq} = \frac{8}{3}\pi^2[U_{22} + (U_{11} + U_{33} + 2U_{13}\cos\beta)/\sin^2\beta]$.

	x	y	z	B_{eq} (Å^2)
Mn(A)	0	0	0	0.242 92
Mn(B)	0.5	0.5	0	0.272 64
C(1)	0.031 06(25)	0.210 61(29)	0.280 60(22)	0.4905
C(2)	0.328 95(25)	0.610 02(29)	0.431 47(22)	0.4583
O(1)	0.096 00(29)	0.100 86(35)	0.206 84(26)	0.4960
O(2)	0.082 74(29)	0.256 96(34)	0.403 54(27)	0.4330
O(3)	0.438 72(29)	0.716 02(36)	0.418 81(27)	0.4806
O(4)	0.216 62(29)	0.649 67(33)	0.494 08(27)	0.5106
O(w1)	0.272 40(28)	0.486 95(35)	0.068 94(27)	0.5309
O(w2)	0.407 91(30)	0.116 84(37)	0.300 36(26)	0.6254
H(1)	−0.078 33(67)	0.274 23(92)	0.234 23(60)	2.5028
H(2)	0.332 53(67)	0.469 31(71)	0.384 48(63)	2.0100
H(3)	0.231 54(61)	0.613 23(71)	0.047 56(61)	1.8000
H(4)	0.202 45(58)	0.399 82(73)	0.013 89(53)	1.6649
H(5)	0.300 08(56)	0.102 50(84)	0.263 18(51)	1.7331
H(6)	0.463 05(61)	0.151 27(73)	0.221 99(51)	1.6779

2.3. Polarized-neutron experiment

Polarized-neutron measurements have been performed on the two-axis diffractometer with lifting counter 5C1, situated on the hot source at the LLB, in Saclay. A polarizing monochromator of $Fe_{0.08}Co_{0.92}$ was used to produce a polarized-neutron beam with a wavelength of 0.73 Å and a polarization equal to 0.98. The flipping efficiency of the cryoflipper device is equal to unity. The sample had a plate-like shape with dimensions 8 mm × 7 mm and a thickness of 3 mm, the b axis being set vertically on the spectrometer.

A vertical magnetic field produced by an electromagnet was applied to the sample. Two data collections have been performed at two different temperatures: above and below the AF three-dimensional ordering of the A ions, at 5.5 K and 2.5 K, respectively. A field of 0.8 T parallel to the b direction was applied for both temperatures.

2.3.1. Above T_N. In the paramagnetic domain ($T = 5.5$ K), magnetic moments are induced on the atoms in the cell by the external field parallel to the b direction. The magnetic structure factor F_M restricted to the manganese contributions is a vector parallel to b with magnitude

$$F_M(hkl) = m_A f_M^A\{1 + \exp[i\pi(k+l)]\} + m_B f_M^B\{\exp[i\pi(h+k)] + \exp[i\pi(h+l)]\} \quad (4)$$

where f_M^A and f_M^B are the magnetic form factors for the hkl reflection, and m_A and m_B the induced moments relative to the A and B ions, respectively. This expression shows that the Mn(A) and Mn(B) moments contribute only to reflections with $k + l$ even. It should be noted that the moments induced on the other atoms in the cell contribute to all types of reflection, giving rise to non-zero magnetic structure factors for reflections with $k + l$ odd. A set of 151 reflections hkl belonging to the reciprocal layers $k = 0$ and 1 without any condition on $k + l$ has been recorded at 5.5 K.

2.3.2. Below T_N. In the antiferromagnetically ordered domain ($T = 2.5$ K), the magnetic structure factor $F_M(hkl)$ relative to the manganese contributions is the sum of four components corresponding to the AF and the weak ferromagnetic moments on A, and to the induced moments on A and B:

$$F_M(hkl) = F_M^{AF} + F_M^F + F_M^i + F_M^B. \quad (5)$$

The component relative to the B ion is a vector parallel to b with magnitude

$$F_M^B(hkl) = m_B f_M^B\{\exp[i\pi(h+k)] + \exp[i\pi(h+l)]\}. \quad (6)$$

The expressions of the components relative to A are the following:

$$\begin{aligned} F_M^{AF} &= \mu_A^{AF} f_M^A\{1 - \exp[i\pi(k+l)]\} \\ F_M^F &= m_A^s f_M^A\{1 + \exp[i\pi(k+l)]\} \\ F_M^i &= m_A^i f_M^A\{1 + \exp[i\pi(k+l)]\} \end{aligned} \quad (7)$$

where μ_A^{AF} is the ordered AF moment and m_A^s the spontaneous ferromagnetic moment on A, the direction of which depends on the magnitude of the applied field $H \| b$. The induced moment m_A^i is directed along b.

Equations (6) and (7) show that the AF component is equal to zero for reflections with $k+l$ even and, in contrast, the ferromagnetic and induced components on Mn(A) and Mn(B) are equal to zero for reflections with $k + l$ odd.

The magnetically ordered phase at 2.5 K in zero field corresponds to the type I represented in figure 2. The AF component is parallel to b and the ferromagnetic component is parallel to c. The application of a magnetic field $H \| b$ induces a transition from type I to type II. For H higher than a field H_c the AF structure factor is a vector belonging to the (a, c) plane and the ferromagnetic structure factor is parallel to b.

2.3.3. Observation of the spin flop. The transition from the type I to the type II structure has been followed by measuring the magnetic structure factor $F_M(100)$ versus field. The (100) reflection does not contain any AF component because of the extinction rule. For the type I structure, the spontaneous ferromagnetic moment is perpendicular to the neutron polarization direction and, as the scattering vector is in the horizontal plane, the scalar product $\boldsymbol{F}_M^{\perp} \cdot \boldsymbol{p}$ is equal to zero. In the type II structure, the spontaneous ferromagnetic moment is collinear with $\boldsymbol{p}$ and contributes in the same way as the induced components on A and B. The magnetic structure factor $F_M(100)$ can be written as a function of the spontaneous and induced moments on A and B, assuming a unique normalized magnetic form factor $f_M(100)$ for both sites of manganese and neglecting the contributions from the non-manganese atoms:

$$F_M(100) = 2f_M(100)(m_A^i - m_B) \qquad H < H_c$$

$$F_M(100) = 2f_M(100)(m_A^s + m_A^i - m_B) \qquad H > H_c.$$

The observation of a discontinuity between 0.35 and 0.38 T gives evidence for the spin flop of the weak ferromagnetic component m_A^s from the c direction towards b. The variation $\Delta F_M = 0.17\mu_B$ at the discontinuity corresponds to a discrete increase of $0.087\mu_B$ for the moment on the A ion, which is in very good agreement with the value of $0.078\mu_B$ found by torque measurement [8].

2.3.4. Data collection at 2.5 K. In order to measure the ferromagnetic distribution alone we restricted our measurements to reflections with $k + l$ even, for which the AF contribution is equal to zero; 92 reflections with $k = 0, 1$ have been collected at 2.5 K.

In the case of hkl reflections with $k + l$ odd, which then contain both AF and nuclear terms, the flipping ratio is not equal to unity for out-of-plane scattering vectors as shown in figure 3(*b*). For example the flipping ratio of the $(-1\,1\,4)$ reflection is equal to 1.004(14) at 5.5 K and becomes 1.208(14) at 2.5 K, owing to the large interfering antiferromagnetic term.

3. Results and discussion

3.1. Fourier summation

The maps given in figure 4 represent the projection of the magnetization density along the direction b, obtained by Fourier summation of the $(h0l)$ magnetic structure factors measured at 5.5 K and 2.5 K, respectively, with $H = 0.8$ T. The induced moment on Mn(B) totally dominates both Fourier maps, the moments induced on the other atoms of the cell being below the limits of uncertainty. The error level of the map is of the order of $0.1\mu_B$ Å^{-2}. The distortions which can be seen out of any atomic positon are due to the lack of about half the Fourier components in the domain $(\sin\theta)/\lambda < 0.67$ Å^{-1}. In the same way, the apparent asphericity of the distribution around Mn(B) is due to the incomplete set of experimental structure factors and has no physical meaning.

3.2. Manganese form factor

On the assumption that the normalized magnetic form factors of the A and B manganese ions are identical, it is possible to simplify equation (4) of the magnetic structure factors

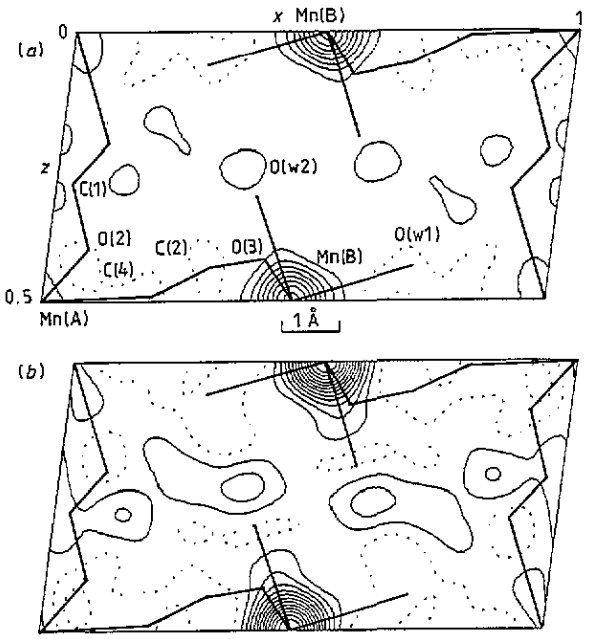

Figure 4. Projection of the magnetization density along the *b* direction, obtained by Fourier summation: (*a*) 58 *h*0*l* reflections measured at 5.5 K; (*b*) 47 *h*0*l* reflections at 2.5 K. The levels start at $\pm 0.1\mu_B$ Å^{-2} with intervals of $0.2\mu_B$ Å^{-2}. Negative contours are shown as broken lines.

of the *hkl* reflections containing contributions from the manganese ions, which means with $k + l$ even only:

$$F_M(hkl) = \begin{cases} 2f_M(hkl)(m_A + m_B) & \text{if } h + k \text{ is even} \\ 2f_M(hkl)(m_A - m_B) & \text{if } h + k \text{ is odd.} \end{cases}$$

The magnetic structure factors of the reflections with $k + l$ even and $h + k$ even or odd, respectively, at 5.5 K are reported as a function of $(\sin\theta)/\lambda$ in figure 5. Good agreement of the ionic Mn^{2+} model with the experimental points is noted. This justifies the fact that the induced moments on the atoms other than manganese are weak enough to be neglected in this form factor analysis. The extrapolation to $(\sin\theta)/\lambda = 0$ yields the value of the sum $m_A + m_B = 2.1\mu_B$ for the reflections with $h + k$ even and of the difference $|m_A - m_B| = 1.35\mu_B$ for the reflections with $h + k$ odd, from which the moments $m_A = 0.38\mu_B$ and $m_B = 1.72\mu_B$ are deduced.

Similarly, at 2.5 K, the following values are obtained for the induced moments on Mn(A) and Mn(B) from reflections with $k + l$ even only, which do not contain any AF contribution: $m_A = m_A^s + m_A^i = 0.3\mu_B$ and $m_B = 3.1\mu_B$.

3.3. Model refinement

In order to extract more detailed information on the magnetization density $\rho(\boldsymbol{r})$ from the magnetic structure factors, it is necessary to define a model for $\rho(\boldsymbol{r})$ and to refine the parameters of this model on the observations. The model is chosen by making the following assumptions.

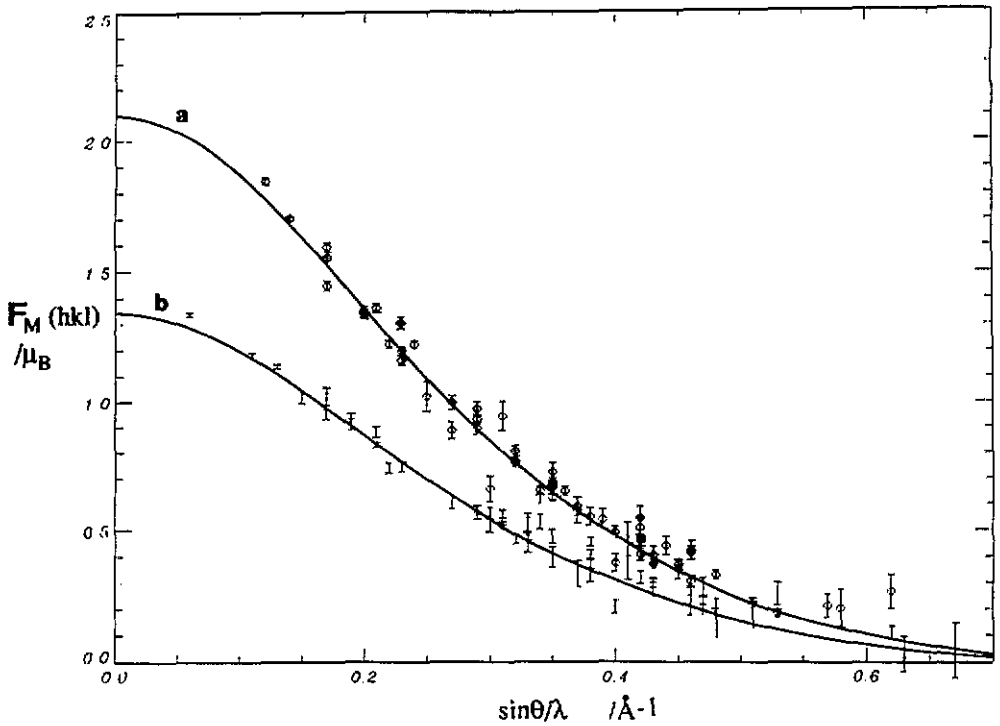

Figure 5. Magnetic structure factors versus $(\sin\theta)/\lambda$ for reflections with $h+l$ even: curve a, reflections with $h+k$ even; curve b, reflections with $h+k$ odd. The full curves correspond to the free-ion Mn^{2+} magnetic form factor scaled in order to fit the experimental data.

(1) The magnetization density is the sum of densities $\rho_i(r_i)$ centred on the atoms in the cell, which are functions of the local atomic coordinates r_i:

$$\rho(r) = \sum_i \rho_i(r_i).$$

(2) The magnetic electrons responsible for the magnetization are located in 3d orbitals on Mn and 2p orbitals on C and O which can be written as the product of a Slater-type radial function and a real spherical harmonic:

$$\phi_{3d}(r_i) = N r_i^2 \exp(-\xi r_i) y_{lm}(\theta_i, \phi_i)$$
$$\phi_{2p}(r_i) = N r_i \exp(-\xi r_i) y_{lm}(\theta_i, \phi_i)$$

where ξ is a Slater exponent and y_{lm} a combination of spherical harmonics:

$$y_{lm} = \begin{cases} (1/2)(Y_{lm+} + Y_{lm-}) & \text{for } m \geqslant 0 \\ (1/2i)(Y_{lm+} - Y_{lm-}) & \text{for } m < 0. \end{cases}$$

The theoretical spin density expressed as a function of the molecular wavefunction is a linear combination of products of the 3d and 2p atomic orbitals. The product of the two Slater functions is also of Slater type and the product of two spherical harmonics is a

spherical harmonic. This why a set of functions $\rho_{lm}(r_i)$, called multipole functions, built up as products of a Slater radial function and a spherical harmonic forms a well-adapted basis set for the analytical description of the spin density [20]:

$$\rho(r_i) = \sum_l \sum_m P_{lm} \rho_{lm}(r_i)$$

with

$$\rho_{lm}(r_i) = N_{lm} r_i^{n_l} \exp(-K\alpha r_i) y_{lm}(\theta_i, \phi_i).$$

The parameters that can be refined are the coefficient K of the Slater exponent α and the multipole populations P_{lm}. The integration of the magnetization density $\rho(r)$ over the unit cell gives simply the sum of the monopole populations P_{00}, because the integral of the multipolar terms with $l > 0$ over the cell is equal to zero. The sum of the populations P_{00} is then equal to the magnetization in the cell and each monopole population yields the value of the induced magnetic moment on the corresponding atom.

The Slater exponents for C and O have been chosen as equal to 2ξ using the value of the exponent ξ calculated for atomic wavefunctions: $\xi = 3.44$ au^{-1} and 4.50 au^{-1}, respectively [21]. The coefficient n_0 is taken to be equal to 2. Instead of using a Slater radial function for the density, it is possible to use directly the magnetic form factor, given as a numerical table, in order to calculate the magnetic structure factors. The 3d magnetic form factor of Mn^{2+} has been used to define the radial part of the monopole on Mn(A) and Mn(B) [22]. A coefficient K has been refined for each Mn atom.

The spin distribution has been refined first in a spherical approximation that means including monopoles only. Considering the very small moments observed on the atoms of the formate bridge, it is not possible to refine the shape of the distribution on these atoms. A more elaborated description has been refined for both manganese ions using the symmetry constraints defined in [23] for local octahedral symmetry. No significant values have been obtained for the refined hexadecapole populations P_{40} and therefore we restricted the model to the spherical description.

3.3.1. Above T_N. The monopole populations obtained by refinement from the set of 151 reflections measured at 5.5 K are given in table 3. At 5.5 K, the induced moment on the paramagnetic B ion is much larger than the moment on A, which has a reduced susceptibility owing to two-dimensional AF interactions in the A layers: Mn(B), $1.73(2)\mu_B$; Mn(A), $0.38(2)\mu_B$. The Mn^{2+} 3d form factor is found to describe very well the radial distribution of the density around both A and B ions. About the same radial extension is found for A and B: $K_A = 0.96(4)$ and $K_B = 0.98(1)$. Significant populations on the formate bridges A–A and A–B, but not on the two water molecules linked to Mn(B), are found by refinement.

In figures 6(*a*) and 6(*b*), we present the induced spin-density maps obtained from the multipole description at 5.5 K, relative to the formate bridge between one A ion and another A ion or a B ion, respectively. The projection of the spin density is drawn along the x direction of the local coordinate system centred on A or B. For site A, the x direction is perpendicular to the O(1)–Mn(A)–O(4) plane and for site B perpendicular to the O(3)–Mn(B)–O(w2) plane.

For both A–A and A–B formate bridges, a positive spin density of the order of $0.01\mu_B$ is observed on the oxygen atoms, while the carbon atom carries negative spin density of the same order of magnitude. Similar trends have been observed for the carbonate group in $MnCO_3$ [24]. The transfer of spin from manganese to the neighbouring oxygen atoms is due

Table 3. Induced magnetic moments at 5.5 and 2.5 K, under an applied field of 0.8 T.

	Magnetic moment (μ_B)	
	$T = 5.5$ K	$T = 2.5$ K
Mn(A)	0.38(2)	0.28(2)
Mn(B)	1.73(2)	3.14(2)
C(1)	−0.017(7)	−0.023(9)
O(1)	0.022(6)	0.014(9)
O(2)	0.015(6)	−0.016(9)
C(2)	−0.011(9)	−0.022(11)
O(3)	0.024(7)	0.025(11)
O(4)	0.013(7)	−0.006(10)
O(w1)		0.018(9)
O(w2)		0.014(10)
Number of reflections	151	92
Number of variables	12	12
Goodness of fit χ^2	1.20	1.10
Agreement R	5.32	2.79

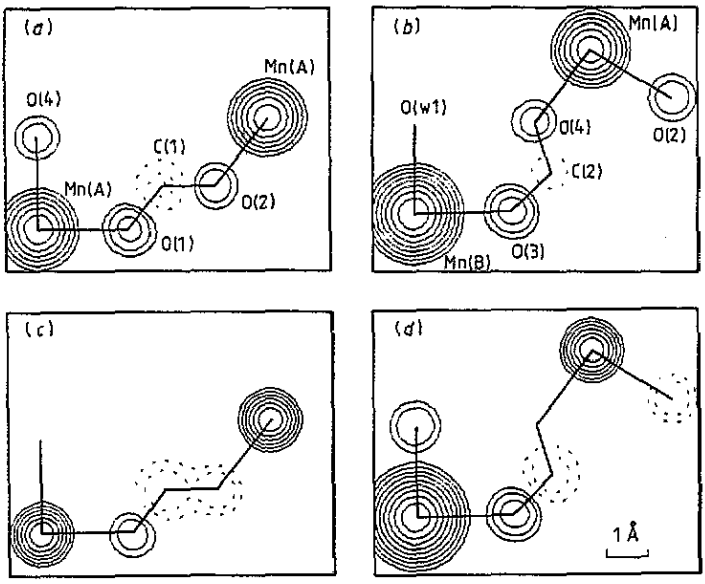

Figure 6. Projection of the magnetization density obtained from multipole refinement at 5.5 K: (*a*) perpendicular to the O(1)–Mn(A)–O(4) plane; (*b*) perpendicular to the O(3)–Mn(B)–O(w2) plane; (*c*) as (*a*), but for 2.5 K; (*d*) as (*b*), but for 2.5 K. The contours are drawn from $-0.005\mu_B$ to $0.025\mu_B$ Å^{-2} with intervals of $0.005\mu_B$ Å^{-2}, and from $0.2\mu_B$ to $0.8\mu_B$ Å^{-2} with intervals of $0.2\mu_B$ Å^{-2}. Negative contours are shown as broken lines.

to covalency. Spin (or exchange) polarization effects of the 2p orbital of carbon belonging to the OCO π bond may be invoked to explain the negative spin density on carbon. The spin transferred to the six oxygen atoms linked to Mn(A) amounts to $0.10\mu_B$, i.e. about

26% of the manganese moment.

3.3.2. Below T_N. At 2.5 K, the A ions are antiferromagnetically ordered, while the B ions are still paramagnetic. Under the applied field of 0.8 T, the AF moments are canted, with the AF component in the (a, c) plane and the weak ferromagnetic component along b as shown in figure 2(b). Magnetic moments are induced on the atoms of the cell along b.

In table 3 are reported the refined values of the induced moments given by the monopole populations obtained from the experimental set of 92 reflections with $k+l$ even, which does not contain any AF contribution. The refinement of the radial extension of the spin density around each manganese atom shows a difference between the A and B sites. The larger coefficient K obtained for A ($K_A = 1.16(7)$) than for B ($K_B = 0.985(5)$) indicates that the spin density is apparently more localized on A than on B, which was not the case at 5.5 K. The observed moment on A, equal to $0.28\mu_B$, is the sum of the spontaneous ferromagnetic component of $0.09\mu_B$ and of the induced moment along b, which is then equal to $0.19\mu_B$.

The spin distribution on the formate groups illustrated in figures 6(c) and 6(d) appears to be perturbed in the magnetically ordered phase. On the A–A bridge, the spin density remains negative on the carbon atom C(1) and positive on the oxygen atom O(1) but becomes negative on O(2). The same trend is observed for the A–B bridge, the spin density remaining negative on C(2) and positive on O(3) linked to Mn(B), while the moment induced on O(4) decreases to zero.

4. Conclusion

Alternate positive and negative induced moments are observed for the formate groups OCO relating the A ions in the A layers as well as for the formate group bridging the A and B layers. The spin distribution on the formate bridge can be explained by covalency and spin (or exchange) polarization effects. The observation of magnetic moments on the C and O atoms of the formate bridges gives clear evidence for the role of the bridges in the magnetic superexchange responsible for the three-dimensional magnetic ordering of the A ions.

References

[1] Osaki K, Nakai Y and Watanabé T 1964 *J. Phys. Soc. Japan* **19** 717
[2] Flippen R B and Friedberg S A 1961 *J. Chem. Phys.* **38** 2652
[3] Abe H, Morigaki H, Matsuura M, Torii K and Yamagata K 1964 *J. Phys. Soc. Japan* **19** 775
[4] Abe H and Torii K 1965 *J. Phys. Soc. Japan* **20** 183
[5] Abe H and Matsuura M 1964 *J. Phys. Soc. Japan* **19** 1867
[6] Bertaut E F, Burlet P and Burlet P 1969 *Solid State Commun.* **7** 343
[7] Skalyo J, Shirane G and Friedberg S A 1969 *Phys. Rev.* **188** 1037
[8] Matsuura M, Koyama K and Murakami Y 1985 *J. Phys. Soc. Japan* **54** 2714
[9] Yamagata K 1967 *J. Phys. Soc. Japan* **22** 582
[10] Ajiro Y 1969 *J. Phys. Soc. Japan* **27** 829
[11] Yamagata K and Abe H 1965 *J. Phys. Soc. Japan* **20** 906
[12] Pierce R D and Friedberg S A 1968 *Phys. Rev.* **165** 680
[13] Burlet P, Burlet P, Bertaut E F, Roult G, de Combarieu A and Pillon J J 1969 *Solid State Commun.* **7** 1403
[14] Koyama K, Terata N and Matsuura M 1982 *J. Phys. Soc. Japan* **51** 2697; 1985 *J. Phys. Soc. Japan* **54** 2708
[15] Gillon B, Cavata C, Schweiss P, Journaux Y, Kahn O and Schneider D 1989 *J. Am. Chem. Soc.* **111** 7124
[16] Radhakrishna P 1982 *J. Physique Coll.* **43** C7 221
[17] Brown P J and Forsyth J B 1981 *J. Phys. C: Solid State Phys.* **14** 5171
[18] Kay M I, Almodovar I and Kaplan S F 1968 *Acta Crystallogr.* B **24** 1312

[19] Zucker U R, Perenthaler E, Kuhs W F, Bachmann R and Schulz H 1983 *J. Appl. Crystallogr.* **16** 358
[20] Brown P J, Capiomont A, Gillon B and Schweizer J 1979 *J. Magn. Magn. Mater.* **14** 289; 1983 *Mol. Phys.* **48** 753
[21] Hehre W J, Stewart R F and Pople J A 1969 *J. Chem. Phys.* **51** 2657
[22] Watson R E and Freeman A J 1961 *Acta Crystallogr.* **14** 27
[23] Holladay A, Leung P and Coppens P 1983 *Acta Crystallogr.* A **39** 377
[24] Brown P J and Forsyth J B 1967 *Proc. Phys. Soc.* **92** 125